CONF-790631--4

SERI/TP-35-254

June 1979

MASTER

# Thermoelectric Ocean Thermal Energy Conversion


T. S. Jayadev
D. K. Benson
M. S. Bohn



**Solar Energy Research Institute**
A Division of Midwest Research Institute

1536 Cole Boulevard
Golden, Colorado 80401



Operated for the
**U.S. Department of Energy**
under Contract No. EG-77-C-01-4042

## DISCLAIMER

## DISCLAIMER

SERI/TP-35-254
UC CATEGORY: UC-64

# THERMOELECTRIC OTEC

T. S. JAYADEV
D. K. BENSON
M. S. BOHN

JUNE 1979



**Solar Energy Research Institute**

1536 Cole Boulevard
Golden, Colorado 80401

A Division of Midwest Research Institute

Prepared for the
U.S. Department of Energy
Contract No. EG-77-C-01-4042

# FOREWORD

This report is an elaboration on a presentation made at the Sixth International Ocean Thermal Energy Conference, Washington, D.C., June 19-22, 1979. It documents work done by the SERI Materials, Systems Analysis, and Solar Thermal Conversion branches on Task 3127. The authors would like to thank Dr. Paul Rappaport for his encouragement during the initial stages of this work. This work has been supported by the Division of Advanced Energy Projects of the Office of Energy Research, U.S. Department of Energy.

T.S. Jayadev
Task Leader

Approved for:

SOLAR ENERGY RESEARCH INSTITUTE

6/4/79
J. C. Grosskreutz
Director for Technology Development

## TABLE OF CONTENTS

## LIST OF FIGURES



## LIST OF TABLES

## NOMENCLATURE

| | |
|---|---|
| $A$ | cross-sectional area of thermoelectric material |
| $A_c$ | cross-sectional area of heat exchanger passage = bW |
| $A_p$ | cross-sectional area of cold water pipe = $\pi d_c^2/4$ |
| $b$ | height of heat exchanger flow passage |
| $C_p$ | fluid (water) specific heat |
| $d_c$ | diameter of cold water pipe |
| $f_p$ | friction factor in cold water pipe |
| $f_{hx}$ | friction factor in heat exchanger flow passage |
| $G$ | mass flow rate in the heat exchanger flow passage ÷ bW |
| $g_c$ | acceleration of gravity |
| $h$ | heat transfer coefficient at fluid/heat exchanger interface |
| $I$ | electrical current in thermoelectric device |
| $K$ | efficiency of thermoelectric material as fraction of Carnot efficiency |
| $k_{te}$ | thermal conductivity of thermoelectric material |
| $k_{eff}$ | effective thermal conductivity of thermoelectric material (see Appendix) |
| $k_p$ | thermal conductivity of the heat exchanger plate material |
| $\ell$ | length of thermoelectric material in an elementary device |
| $L$ | length of heat exchanger flow passage in flow direction |
| $L_c$ | length of cold water pipe |
| $\dot{m}$ | mass flow rate in heat exchanger flow passage |
| $\dot{m}_c$ | total mass flow rate of cold water |
| $N$ | total number of flow passages in the heat exchanger |
| NGU | number of generation units |
| $P''_e$ | local electrical power generation per unit base area of heat exchanger |
| $P_c$ | electrical power generated by a flow channel |
| $P_{hx}$ | power required to pump fluid through a flow passage |
| $P_p$ | power required to pump fluid through the cold water pipe |
| $P_o$ | net electrical power produced by the system |
| $P''_o$ | maximum value of $P_o$ (wrt G) per unit heat exchanger plate area |
| Pr | fluid Prandtl number |
| $q$ | heat flux in thermoelectric device |

| | |
|---|---|
| $q_h$ | heat transferred per unit area from hot fluid to cold fluid |
| R | electrical resistance of thermoelectric device |
| $R_f$ | thermal resistance from the fluid to the thermoelectric material (including plate resistance and fouling) |
| $R_{te}$ | thermal resistance of the thermoelectric material including Peltier resistance |
| Re | Reynolds number in heat exchanger flow passage |
| t | thickness of heat exchanger plate |
| $t_{te}$ | thickness of thermoelectric material |
| $T_\ell$ | cold junction temperature of the thermoelectric |
| $T_h$ | hot junction temperature of the thermoelectric |
| $T_{hot}$ | temperature of the hot fluid |
| $T_{cold}$ | temperature of the cold fluid |
| U | thermal conductance from the hot fluid to the cold fluid |
| V | voltage generated by an elementary thermoelectric device |
| W | width of heat exchanger flow passage |
| $\alpha$ | Seebeck coefficient of thermoelectric material |
| $\beta$ | fraction of area covered by thermoelectric material |
| $\Gamma$ | heat exchanger effectiveness parameter (Eq. 12) |
| $\sigma$ | electrical conductivity of thermoelectric material |
| $\varepsilon$ | Carnot efficiency |
| $\eta_p$ | efficiency of water pumps |
| $\mu$ | fluid viscosity |
| $\rho$ | fluid density |
| $\Delta\rho$ | $\rho(T_{cold}) - \rho(T_{hot})$ |

## ABSTRACT

A novel thermoelectric OTEC concept is proposed and compared with the ammonia closed-cycle designs. The thermoelectric OTEC is a much simpler system which uses no working fluid and therefore requires no pressure vessel, working fluid pumps, or turbogenerator. These components are replaced by power modules which are heat exchangers integrated with thermoelectric generators.

The thermoelectric OTEC offers several potential advantages including: simpler and more easily mass-produced components; higher reliability system performance through the use of a high level of redundancy and long-lived, solid-state thermoelectric generators; greater safety for crew and environment by elimination of the pressurized working fluid; and the possibility of lower system costs.

These comparisons are discussed and plans for future work are presented in the paper.

THIS PAGE INTENTIONALLY LEFT BLANK

## SECTION 1.0

## INTRODUCTION

Over the past few decades, the art and science of thermoelectric energy conversion has gradually evolved to a high level of performance. Thermoelectric generation has become the preferred method for producing electric power where reliability and maintenance-free operation are essential. Radioisotope-heated thermoelectric generators power orbiting satellites, remote radio transmitters, space probes (Pioneers 10 and 11 and Viking Mars Landers), deep sea sonar sounding buoys, etc. Fossil-fueled thermoelectric generators provide reliable cathodic corrosion protection for remote pipelines, bridges, etc., and large-scale industrial thermoelectric cooling is becoming a commercial reality in France [1].

The objective of an extensive thermoelectrics R&D program during the 1960s was to develop materials and systems which were competitive with the steam turbogenerator. Although this goal was never met and thermoelectric research suffered a decline, it is important to recognize that thermoelectrics were judged by a comparison with steam turbines in the temperature range where steam is most efficient and economical. For much lower temperature heat sources, steam turbines are much less efficient and economical, and mass-produced thermoelectric generators can compete very favorably.

A major reservation about thermoelectric devices during the 1960s was degradation of the materials and bonds under high temperature thermal cycling. This problem does not exist at low temperatures such as those encountered in the thermoelectric OTEC. Low temperature thermoelectric devices have exhibited 35 year mean time between failures [2].

New materials now being developed by the thermoelectrics industry exhibit energy conversion efficiencies far superior to presently available thermoelectric materials. These new materials may represent a major improvement in thermoelectric technology and may offer possibilities for numerous new applications. The thermoelectric OTEC is one such new application that has been proposed by the authors and is now undergoing preliminary evaluation at SERI.

THIS PAGE INTENTIONALLY LEFT BLANK

# SECTION 2.0

# DISCUSSION

## 2.1 BASIC PRINCIPLES

The thermoelectric OTEC is a simple system that uses a thin layer solid-state generator rather than a working fluid. Consequently, no evaporator, condensor, working fluid pump, pressure vessel, or turbogenerator is required (Fig. 2-1). A compact heat exchanger is used to transmit heat through the thermoelectric generator.

Thermoelectric generation makes use of a bulk phenomenon--the Seebeck effect (the same phenomenon that makes a thermocouple operate). A temperature gradient across any material tends to drive charge carriers from the hot side to the cold side and produce a voltage, V, which is proportional to the temperature difference, $\Delta T$. The proportionality constant, the Seebeck coefficient, is a characteristic of the material:

$$\alpha = \frac{V}{\Delta T} \tag{1}$$

For most metals $\alpha$ is quite small, a few microvolts per degree, but specially designed semiconductor thermoelectric alloys produce several hundred microvolts per degree Kelvin. Using such materials, thermal energy can be converted to electrical energy at about 20% of the maximum (Carnot) theoretical efficiency.

Efficient thermoelectric materials exhibit a high Seebeck coefficient $\alpha$, high electrical conductivity $\sigma$, and low thermal conductivity k. A figure of merit,

$$Z = \frac{\alpha^2 \sigma}{k} \tag{2}$$

is a good indicator of a thermoelectric material's performance. Fig. 2-2 shows how Z varies with temperature for the most common commercial thermoelectric materials [3]. Special alloys of bismuth, antimony, tellurium, and selenium now used in the thermoelectric cooling industry have Z values as high as $3.5 \times 10^{-3}$ at room temperature. Notice that the highest figures of merit occur in the temperature range of interest for OTEC.

New alloys of bismuth, antimony, and tellurium, which are under development by the industry, have recently exhibited reproducible values of $Z = 6 \times 10^{-3}\ K^{-1}$. Such materials could provide a conversion efficiency as high as 30% of the Carnot limit. In a thermoelectric OTEC, the use of such an advanced material could produce a gross conversion efficiency of 2%--an efficiency comparable to the closed cycle ammonia OTEC. Other new materials such as amorphous semiconductors and organic semiconductors also have promise for achieving high thermoelectric energy conversion efficiency in the OTEC temperature range.

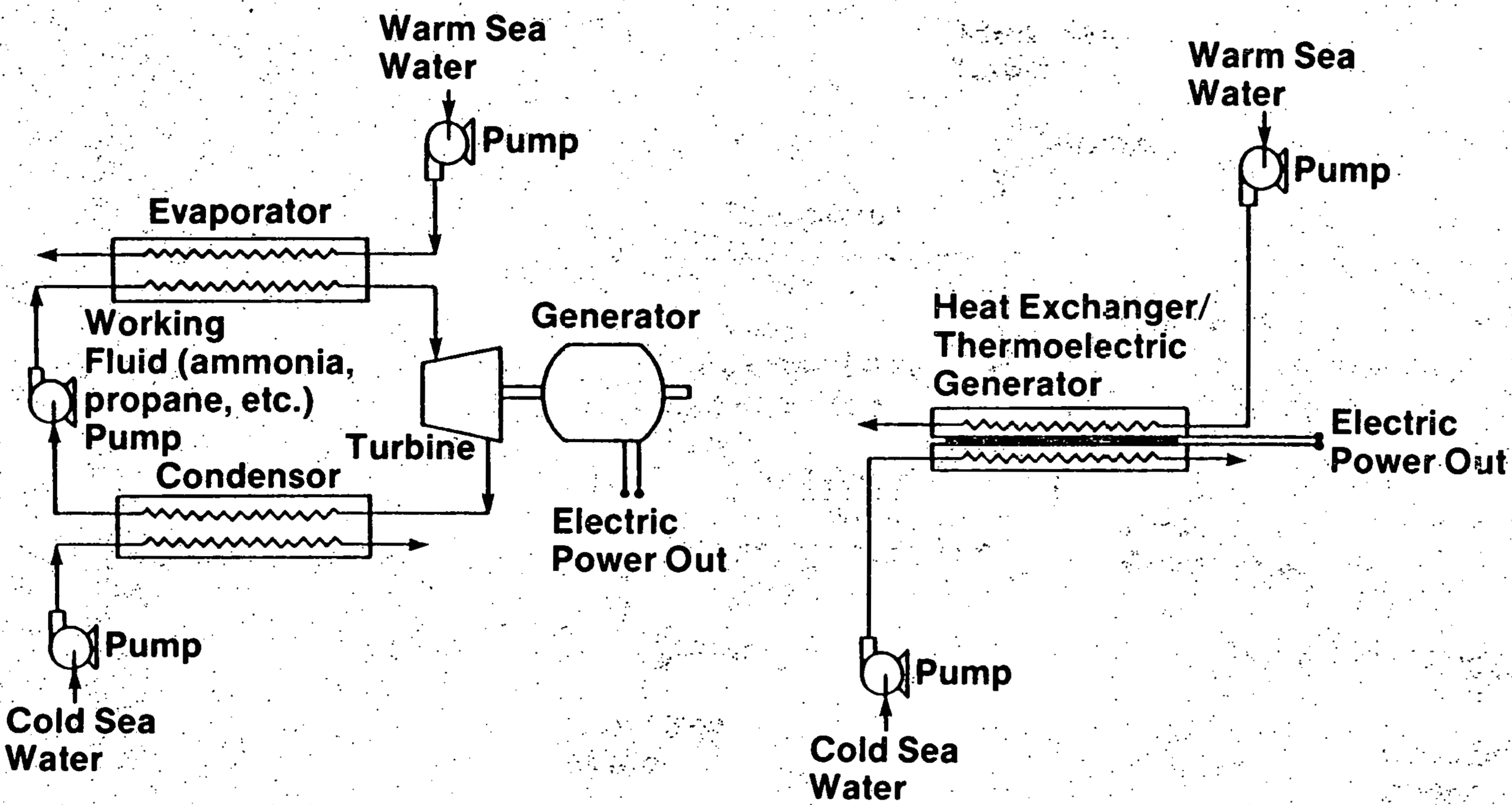


A. Schematic Closed Cycle OTEC

B. Schematic Thermoelectric OTEC

**Figure 2-1. Comparison of System Schematic Designs for Closed Cycle OTEC and Thermoelectric OTEC**

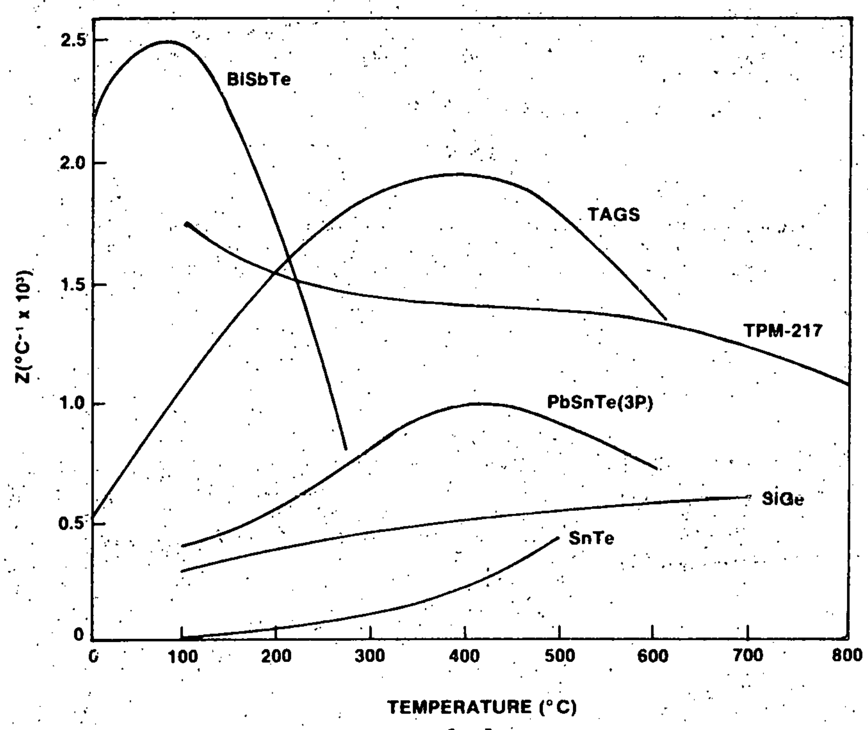


**(a)**

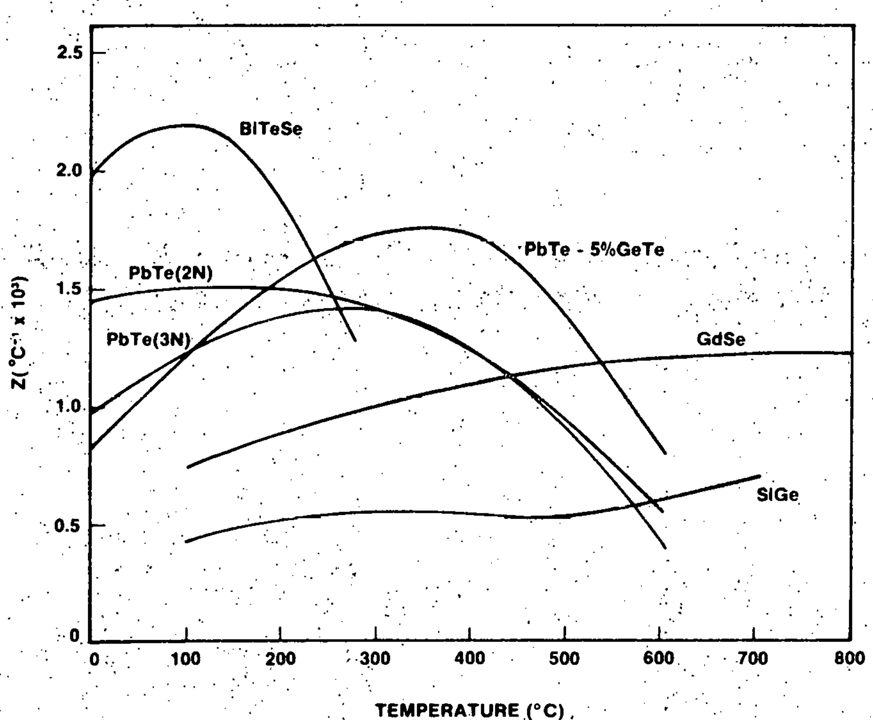


**(b)**

**Figure 2-2. Figure of Merit of Thermoelectric Alloys: (a) p-Type Alloys; (b) n-Type Alloys**

## 2.2 HEAT EXCHANGER AND THERMOELECTRIC GENERATOR

The thermoelectric OTEC concept permits the use of a particularly simple design for the power module which serves as both heat exchanger and electric power generator.

Figure 2-3 shows a preliminary design concept for such a module which would produce about 30 $kW_e$ (net) in an OTEC with $\Delta T = 20$ K [4]. If advanced thermoelectric materials were used, the net output from the module could be increased by about 50%. A 400 $MW_e$ (net) plant would use about 20,000 such modules.

The power module is basically a heat exchanger of parallel plate design with the thermoelectric generators sandwiched between the flow channels as shown. The material of choice in the heat exchanger is a copper-nickel alloy which can provide several advantages:

- excellent resistance to biofouling,
- low corrosion rate (less than $2.5 \times 10^{-5}$ m/yr or 1 MPY [5]),
- high thermal conductivity,
- high electrical conductivity, and
- easy fabrication.

Unlike the closed-cycle OTEC designs, the thermoelectric OTEC is forgiving. For example, a corrosion pit which would shut down an ammonia OTEC module (because of concern for accelerated corrosion and/or scaling) would damage only a small number of thermoelectric elements; it would not diminish the power output from the affected power module perceptibly and would not require repair. One of the consequences of this forgiving design is that only minimal corrosion tolerances need be used in the heat exchanger.

The thermoelectric generator device is a novel design which makes use of thick-film technology already well developed in the electronics industry. The thermoelectric material could be deposited on the copper base as a paste by lithographic techniques and fired in place to form a durable coating; a suitable pottant could be added to fill the interstices, and finally the cover plate could be soldered in place. All of these steps are amenable to automation.

The themoelectric generator design is particularly simple because only a single type (that is either n-type or p-type) semiconductor need be used. Each themoelectric generator device will then consist of many identical thermoelectric elements connected in parallel, and these devices in turn will be interconnected in series to provide a high current, low voltage power module. Modules can be suitably insulated from each other and connected in series-parallel arrays as needed to produce the desired system current and voltage output [4].

The particularly simple design of the thermoelectric power modules suggests that they may be suitable for large-scale, automated mass production. This possibility is in contrast to the present tube-in-shell heat exchanger designs for closed cycle OTEC, which require expensive, labor intensive assembly.

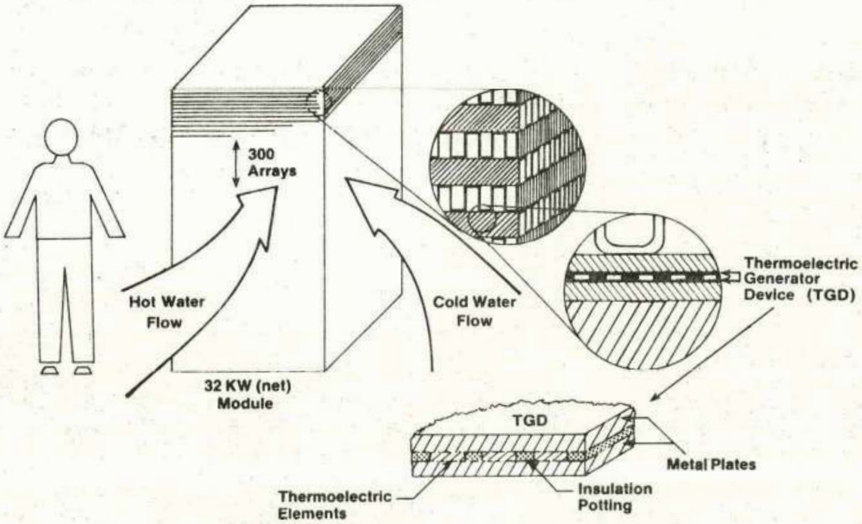


**Figure 2-3. Preliminary Power Module Design**

(This early design utilizes a cross-flow, plate and fin heat exchanger. Later analyses showed that parallel plate heat exchanger performance was comparable.)

## 2.3 ENVIRONMENT AND SAFETY

The ammonia closed-cycle OTEC poses several safety and environmental risks that would not be present with a thermoelectric OTEC. Small, chronic leaks of ammonia may pose a health hazard to the operating crew and cause accelerated corrosion and scaling of the heat exchangers. Larger leaks, which would release large quantities of ammonia before they could be repaired, would be a serious health hazard, a potential fire and explosion hazard, and have serious impacts on marine life (particularly in combination with hypochlorite used to control biofouling).

The thermoelectric OTEC would have none of the hazards of ammonia, but its use of copper alloy heat exchangers would significantly raise the copper and nickel ion concentrations near the OTEC plant. These ions are harmful to certain mollusks. However, a study of the problem has shown that the copper and nickel ion concentrations probably would not exceed the EPA standards for marine water quality [6].

## 2.4 HEAT EXCHANGER DESIGN

To determine the performance which could be expected from a thermoelectric OTEC system, a preliminary performance analysis was made of a simplified design. Included in the analysis was development of an expression for electrical power output per unit base area of the heat exchanger, selection of the correct thickness of thermoelectric material, calculation of parasitic losses, and minimization of costs for a given plant output power.

The heat exchanger considered has parallel flow channels of rectangular cross section (Figs. 2-3 and 2-4). Cold water and hot water are pumped through alternate flow channels with thermoelectric material sandwiched between the channels.

The power output of the thermoelectric module per unit area may be written*

$$P''_e = Kq_h\left(1 - \frac{T_\ell}{T_h}\right) \tag{3}$$

The heat transferred from the hot fluid to the cold fluid is

$$q_h = \frac{T_{hot} - T_{cold}}{R_{te} + 2R_f} = \frac{T_h - T_\ell}{R_{te}} \tag{4}$$

The power output may be expressed in terms of the various thermal resistances [Eq. 3] by replacing $T_\ell$ and $T_h$ in Eq. 4 and rewriting it as:

---

*Nomenclature is defined in the Nomenclature section of this report, preceding the Abstract.

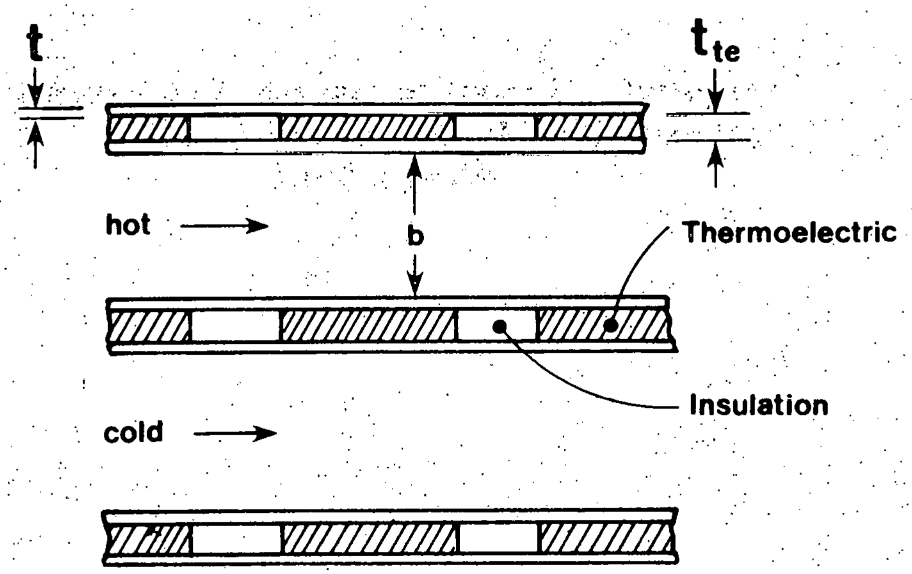


**Figure 2-4. Detail of Heat Exchanger/ Thermoelectric Generator Configuration**

$$P_e'' = \frac{KR_{te}}{T_{hot} - R_f\left(\frac{T_{hot} - T_{cold}}{2R_f + R_{te}}\right)} \left(\frac{T_{hot} - T_{cold}}{2R_f + R_{te}}\right)^2 \qquad (5)$$

Since the temperature differences are small,

$$\varepsilon = 1 - \frac{T_{cold}}{T_{hot}} \ll 1 \qquad (6)$$

Equation 5 can be linearized to give

$$P_e'' = \frac{K\varepsilon^2 T_{hot}}{R_{te}(1 + 2R_f/R_{te})^2} \qquad (7)$$

The local electric power generation $P_e''$ may be maximized by adjusting the thermal resistance of the thermoelectric to $R_{te} = 2R_f$, giving

$$P_e'' = \frac{K\varepsilon^2 T_{hot}}{8R_f} \qquad (8)$$

The power density $P_e''$ is a function of distance along the flow direction within the passage ($T_{hot}$ and $T_{cold}$ vary in the flow direction) and must be integrated along the flow length to determine power output per flow channel. This calculation is similar to determining heat exchanger effectiveness as a function of NTU (number of transfer units) for a given flow configuration [7]. However, since $P_e''$ is proportional to the square of the temperature difference, the calculation of power generation per flow passage must be carried out for each flow configuration; and the results of heat exchanger effectiveness calculations are not useful. This power generation calculation was done for a parallel flow and a counter flow arrangement, and the results show that NTU for power generation is four times that for heat transfer. Therefore the number of generation units NGU can be defined as

$$NGU = \frac{4ULW}{C_p \dot{m}} = \frac{L}{GC_p R_f b} \qquad (9)$$

In addition, for small values of NGU (~1) the flow configuration is not important in determining the power generation per flow channel and the change in fluid temperatures is small.

For NGU << 1 the power generation of a flow channel is

$$P_c = P_e'' WL \qquad (10)$$

but as NGU increases, the power generation of the channel per unit channel length decreases as [1-exp(-2NGU)]/2NGU. In general we found that for NGU < 0.7 this expression was valid for parallel flow or counterflow heat exchangers, and we expect it will also be valid for most other flow arrangements.

The power generated by the channel is given by

$$P_c = \frac{0.95\ \Gamma K \varepsilon^2\ T_{hot}\ WL}{8R_f} \qquad (11)$$

where $\Gamma = \frac{1-\exp(-2NGU)}{2NGU}$ (12)

The factor 0.95 accounts for an expected 5% loss due to electrical contact resistance at the heat exchanger/thermoelectric junction.

Pumping the fluid through the flow channel requires pumping power [8]:

$$P_{hx} = f_{hx} \frac{L}{b} \frac{G^3 bW}{\rho^2 g_c} + \text{minor losses}$$

$$f_{hx} = 0.079\ Re^{-1/4} \qquad (13)$$

$$Re = \frac{2bG}{\mu}$$

If the cold water pipe feeds N/2 heat exchanger channels, a pumping power $P_p$ will be required:

$$P_p = f_p \frac{L_c}{d_c} \frac{(GbWN/2)^3}{2\rho^2 g_c A_p^2} + L_c \frac{\Delta\rho}{\rho} \frac{GbWN}{4} + \text{minor losses} \qquad (14)$$

The first term in Eq. 14 is the frictional loss, while the second term is the work required to pump the cold water up against the density gradient.

The cold water pipe Reynolds numbers are on the order of $10^8$, and we may assume fully turbulent flow. Assuming a dimensionless roughness for a cold water pipe of 0.0003 gives $f_p = 0.015$. The density gradient term was derived by neglecting compressibility and salinity effects and by assuming a linear density profile with depth. Minor losses refer to losses in channel inlets or outlets.

Assuming the pumping power can be supplied with efficiency $\eta_p$, the net power output of a plant consisting of N channels is

$$P_o = NP_c - \frac{1}{\eta_p}(P_p + NP_{hx}) \qquad (15)$$

We have neglected power required to pump the warm water to the heat exchanger inlet.

Dividing Eq. 15 by 2NWL, we find the net output power per unit heat exchanger plate area:

$$P_o'' = \frac{P_c}{2WL} - \frac{1}{\eta_p}\left(\frac{P_p}{2NWL} + \frac{P_{hx}}{2WL}\right) \tag{16}$$

Proper heat exchanger design will minimize the pumping and material requirements. The parameters which we may vary most easily are the flow rate G and the heat exchanger flow length L (or NGU). The heat exchanger Reynolds number has a weak influence on the design except for determining the plate spacing b, which is constrained by cleaning requirements. The length of the cold water pipe is determined by the depth required to reach the desired cold water temperature, and the diameter of the cold water pipe is probably limited to a maximum of about 40 m because of fabrication and deployment difficulties.

The heat exchanger is designed by varying G and NGU with a Reynolds number which gives a reasonable b until minimum material and pump costs result. The thermal resistance $R_f$ is given from reference 8.

$$R_f = \frac{1}{h} + \frac{t}{k_p} + R_{foul} \tag{17}$$

$$h = 0.023\ Re^{-1/5}\ GC_p Pr^{-2/3} \tag{18}$$

The power density $P_o''$ may then be calculated and the required area 2NWL can be found, given the required plant output power. The mass flow of (hot plus cold) water is $(Gb/2L)\ (P_o/P_o'')$ and the required thickness of thermoelectric material can be found from $R_{te} = 2R_f$ (see Appendix).

The power modules will require an area of 2NWL of heat exchanger plates and thermoelectric device plates, and an area of NWL of thermoelectric material.

We assumed the following values:

$T_{hot} = 298°K$, $T_{cold} = 278°K$

Properties of fresh water at 20°C

$L_c = 914$ m

$K = 0.2$

$\eta_p = 0.8$

$\Delta\rho/\rho = 0.0029$

Minor losses:

| | |
|---|---|
| Coldwater pipe inlet | = 0.04 (dynamic head loss) |
| Cold water pipe manifolding | = 0.04 |
| Pump ducting to heat exchangers | = 0.10 |
| Heat exchanger inlet | = 0.38 |
| Heat exchanger outlet | = 0.56 |

$\beta = 0.3$

$R_{foul} = 0.35$ °C-cm²/W

$t = 0.51$ mm

$k_p = 0.433$ W/cm°C

The optimization procedure for a net 400 $MW_e$ yields:

$b = 1.3$ cm

$G = 80$ g/cm$^2$s

$L = 10.32$ m (NGU = 0.6)

$t_{te} = 1.97\beta$ mm

$d_c = 40.5$ m

Required area of heat exchanger plate = $26.38 \times 10^6$ m$^2$

Required flow rate (hot plus cold) = $13.28 \times 10^6$ kg/s

## 2.5 COST ESTIMATES

The economics of the thermoelectric materials presently considered for OTEC benefit from two factors. The elements involved (mainly bismuth and tellurium) are byproducts of lead, gold, and copper processing, and they are available in abundance [4].

Since the mining costs and most of the processing costs are borne by the primary products, the byproduct costs are determined by the costs of capital equipment, operation, and maintenance of the byproduct separation and purification process. At present, these costs must be recovered with the sale of a relatively small volume of byproduct. As larger quantities are demanded, production equipment can be scaled up, its efficiency improved, and its costs spread over a larger volume of byproduct. The result of this situation is an inverted supply-demand curve. The greater the demand, the lower the unit costs.

Information obtained from a major producer of bismuth and tellurium indicates very substantial reduction in material costs as the demand increases [3]. The following trend is predicted for the price of $Bi_2Te_3$:

| Demand | Unit Cost (1979 $/lb) |
|---|---|
| $10^3$ | 2.96 |
| $10^4$ | 2.37 |
| $10^5$ | 1.78 |
| $10^6$ | 1.19 |

The conceptual design for a thermoelectric OTEC is not yet well enough developed to justify any attempt at making detailed cost estimates. However, it is possible to make an order of magnitude estimate of the system costs for comparison with closed cycle system estimates.

Two major subsystems probably account for most of the thermoelectric OTEC cost--the power modules (heat exchanger-thermoelectric generator combination) and the seawater pumps. With automated mass production, the power modules should approach about 1.35 times the cost of the materials required. Seawater pumps for OTEC have been surveyed and an algorithm developed relating cost to pumping capacity [9,10]:

$$\text{Cost per unit capacity} = 313\ Q^{-0.616} \tag{19}$$

where Q is $m^3/s$ of seawater and costs are given in thousands of 1979 dollars per $m^3/s$ capacity.* Utilizing these simplifying assumptions, the approximate costs are estimated as follows.

The thermoelectric generator for the 400 $MW_e$ (net) plant discussed in the preceding section produces about 30 $W/m^2$ net power. The power module surface area required is $1.3 \times 10^7$ $m^2$. The masses of the required materials are estimated as the product of their density and thickness times the total heat exchanger area [4]:

- flow channel plates of 90 copper - 10 nickel alloy with thickness $0.508 \times 10^{-3}$ m (0.02 in.) and density 8900 $kg\text{-}m^{-3}$ (8.9 $g\text{-}cm^{-3}$): mass = $8900 \times 0.508 \times 10^{-3} \times 1.3 \times 10^7 = 5.9 \times 10^7$ kg ($267 \times 10^6$ lb).
- thermoelectric device plate of copper with thickness $0.13 \times 10^{-3}$ m (0.005 in.) and density 8900 kg - $m^{-3}$ (8.9 g - $cm^{-3}$): mass = $8900 \times 0.13 \times 10^{-3} \times 1.3 \times 10^7 = 15 \times 10^6$ kg ($33 \times 10^6$ lb).
- thermoelectric material covering 0.30 of the surface area and a thickness of $0.59 \times 10^{-3}$ m and density 7700 $kg\text{-}m^{-3}$ (7.7 $g\text{-}cm^{-3}$): mass = $0.59 \times 10^{-3} \times 7700 \times 0.30 \times 1.3 \times 10^7 = 1.77 \times 10^7$ kg ($39 \times 10^6$ lb).

Two flow channel plates and two thermoelectric device plates are required for each unit of power module area. Materials requirements and cost are summarized in Table 2-1.

The pumping capacity for a 400 $MW_e$ thermoelectric OTEC is $1.33 \times 10^4$ $m^3/s$. In the interest of increased reliability through a high level of redundancy, it may be desirable to use 66 large pumps of 200 $m^3/s$ capacity each. The algorithm (Eq. 19) yields a cost of $\$2.4 \times 10^6$ per pump or a total pump cost of $\$158 \times 10^6$ or $\$395/kW_e$ net electric power.

It is important to note the sensitivity of the thermoelectric OTEC costs to thermoelectric conversion efficiency. The power density achievable is proportional to the 3/2 power of the conversion efficiency, so that if the advanced materials now under development were used in these estimates instead of current, commercial thermoelectric materials, all of the costs would be multiplied by a factor $(\text{efficiency old}/\text{efficiency new})^{3/2}$, which equals $(0.2\ \text{Carnot}/0.3\ \text{Carnot})^{3/2} = 0.54$. Thus, the successful development of the new, more efficient thermoelectric materials will have a strong effect on the economics of this concept. Similarly, the development of a more corrosion resistant copper alloy for the heat exchanger could reduce materials requirements and costs dramatically. The capital cost estimates are listed in Table 2-2. The greater simplicity and reliability of the thermoelectric OTEC should

*1977 dollars were inflated to 1979 dollars by using the Chemical Engineering Plant Cost Index [11].

have a favorable influence on the life cycle costs: fewer replacements or major repairs of rotating machinery, fewer costly biofouling control measures, larger availability factor, etc. These improvements may offset any initial capital cost disadvantages.

**Table 2-1. SUMMARY OF POWER MODULE MATERIALS REQUIREMENTS AND COSTS FOR A 400 $MW_e$ (NET) THERMOELECTRIC OTEC**

| Component | Material Required ($10^6$ kg) | Material Required ($10^6$ lb) | Unit Cost ($/kg) | Total Cost ($10^6$ $) |
|---|---|---|---|---|
| Heat exchanger channel plates (90 copper - 10 nickel alloy) | 118 | 260 | 2.2 | 260 |
| Thermoelectric device (copper plates) | 30 | 66 | 1.8 | 54 |
| Thermoelectric material (alloyed $Bi_2Te_3$) | 18 | 40 | 2.6 | 47 |
| | | | Total materials cost = | 361 |
| Total materials cost x 1.35 = fabricated power module costs = | | | | 487 |
| | | | Cost per $kW_e$ net power = | $1218 |

[a]Costs estimated from current (1979) commodity prices for electrolytic copper ($0.75/lb) and nickel ($2.20/lb) with 1.10 multiplier to cover alloy processing [12].

## 2.6 POTENTIAL MARKET PENETRATION

The preliminary nature of the cost estimates for thermoelectric OTEC do not warrant a detailed market penetration study at present. However, it is possible to estimate the relative impact of reduced OTEC capital costs on its probable market penetration.

The MITRE system for Projecting the Utilization of Renewable Resources (SPURR Model) [13] was used to compare OTEC base load power systems with various capital costs against conventional power sources and other solar options. The market was limited to the southern United States; OTEC sites were limited to the Gulf of Mexico. Figure 2-5 shows the resulting projections through the year 2000. Notice that even a small decrease in OTEC capital costs below the base case cost range ($1371-$2020/$kW_e$, 1979 dollars) can dramatically improve the market penetration. Such projections offer encouragement to our efforts to design a lower cost thermoelectric OTEC.

Table 2-2. ULTIMATE CAPITAL COST ESTIMATES FOR OTEC SYSTEMS (400 $MW_e$ PLANT)

| | Ammonia Closed Cycle[a] | | Thermoelectric OTEC | |
|---|---|---|---|---|
| Module | Aluminum HX (1979 $/kW) | Titanium HX (1979 $/kW) | Commercial Thermoelectrics (1979 $/kW) | Advanced Thermoelectrics (1979 $/kW) |
| Heat exchangers (and thermoelectrics) | 482-844 | 567-989 | 1218 | 658 |
| Demisters | 8-48 | 8-48 | NA | NA |
| Turbogenerators | 84-135 | 84-135 | NA | NA |
| Seawater pumps | 103-241 | 115-241 | 395 | 213 |
| Other power systems | 139-235 | 130-235 | 130-235 | 130-235 |
| Platform | 60-362 | 60-362 | 60-362 | 60-362 |
| Cold water pipe | 86-96 | 86-96 | 86-96 | 86-96 |
| Mooring/deployment | 60-238 | 60-238 | 60-238 | 60-238 |
| Electric cable | 121-543 | 121-543 | 121-543 | 121-543 |
| Total | 1143-2743 | 1232-2887 | 2070-2722 | 1326-2343 |
| Average | 1943 | 2064 | 2396 | 1835 |

[a]On a module basis, these represent the highest and lowest estimates by four DOE contractors and DOE personnel as reported during February 1978. The contractors' names corresponding to the estimates made are priority information and are not presented for that reason. These estimates are for sites 3 miles to 200 miles from shore [13]. Costs have been inflated to 1979 dollars using the Chemical Engineering Plant Cost Index and ref. [11].

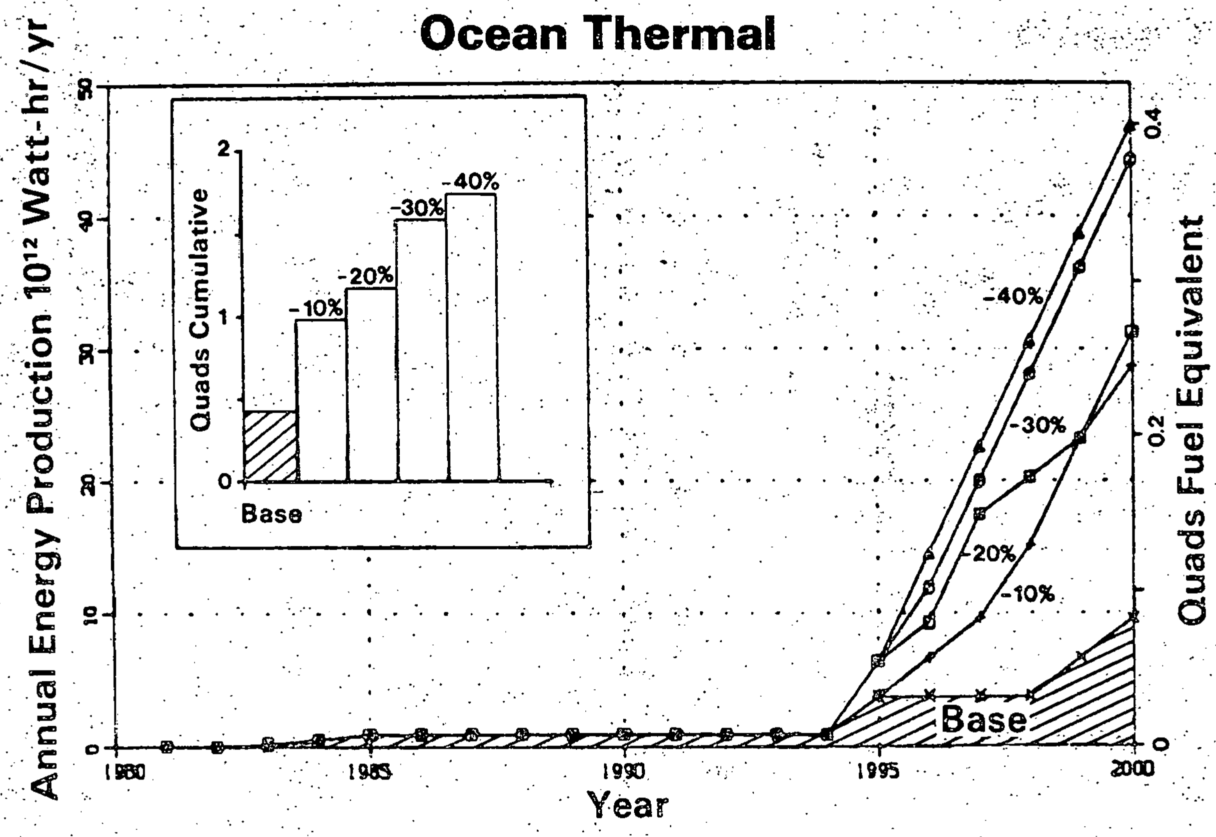


**Figure 2-5. The Market Penetration of Ocean Thermal Electric Systems Based on the Results of a Simulation Model (14)**

THIS PAGE INTENTIONALLY LEFT BLANK

## SECTION 3.0

## CONCLUSIONS

The concept of a thermoelectric OTEC offers many advantages in simplicity, reliability, and safety. Its economic competitiveness appears to depend on successful development of new thermoelectric materials and power module designs. The potential for decreased OTEC costs and increased market penetration are promising.

Ongoing SERI research will include continued evaluation of newly developed thermoelectric materials and research to discover additional thermoelectrics among new classes of materials such as amorphous and organic semiconductors. Thermoelectric device design and fabrication R&D and new systems concepts for integrating the heat exchangers and thermoelectrics are also being pursued. Further analysis of the thermoelectric OTEC and other potential solar applications are in progress.

THIS PAGE INTENTIONALLY LEFT BLANK

# SECTION 4.0

## REFERENCES


1. Stockholm, J. G. et al. (Air Research Industries, Paris, France). "Large Scale Thermoelectric Cooling." Proceedings of the Second International Conference on Thermoelectric Energy Conversion, Dallas, TX, March 1978.

2. Goff, J. F. (Naval Surface Weapons Laboratory). Thermoelectric Materials for Energy Conversion Devices. Naval Ordinance Laboratory Technical Report 74-166, June 1974.

3. Neill, J. M.; Elsner, N. B.; and Sonn, D. L. Thermoelectric Applications to Solar Energy. General Atomic Corp. Report C15168, November 1978.

4. Jayadev, T. S. et al. Conversion System Overview Assessment, Part I. Solar Thermoelectrics. Solar Energy Research Institute Report TR-35-078 (in preparation).

5. Czikk, A. M. et al. Ocean Thermal Power Plant Heat Exchangers. Linde Division, Union Carbide Corp. ERDA/NSF Report 43441-76/2, May 1976.

6. Ocean Thermal Energy Conversion - Environmental Development Plan, U.S. Dept. of Energy, DOE/EDP-0006, pp. 11-13, March 1978.

7. Kays, W. and London, A. L. Compact Heat Exchangers. McGraw Hill, Inc., New York, 1964.

8. Solano, J. G.; Mack, W. M.; and Rohsenhow, W. M. "Performance Ranking of Plate-Fin Heat Exchanger Surfaces." Transactions of the ASME, Vol. 100, August 1978, pp. 514-519.

9. Little, T. E. et al. Deep Water Pipe, Pump, and Mooring Study, Ocean Thermal Energy Conversion Program Final Report, Westinghouse Electric Corp., Oceanic Division, June 1976.

10. Bartone, L. M., Jr. (Gilbert/Commonwealth, Energy Research Division), "Alternative Power Systems for Extracting Energy from the Ocean: A Comparison of Three Concepts," Proceedings of the Fifth Ocean Thermal Energy Conversion Conference, Vol. VII, A. Lavi, ed., February 20-22, 1978, Miami Beach, FL, September 1978, pp. 68-108.

11. Mascio, N. E. "Predict Costs Reliably via Regression Analysis." Chemical Engineering, February 12, 1979, pp. 115-121.

12. Chemical Marketing Reporter, April 23, 1979.

13. Curto, P. A. (Metrek Division of Mitre Corp.), "An Update of OTEC Baseline Design Costs," Proceedings of the Fifth Ocean Thermal Energy Conversion Conference, Vol. II, September 1978, pp. 77-93.

14. Rebibo, K. et al. "A System for Projecting the Utilization of Renewable Resources, SPURR Methodology," Metrek Division, Mitre Corp., ERDA Report ERHQ/2322-77/4, September 1977.

## APPENDIX

The effective thermal conductivity in a thermoelectric generator can be expressed simply as a combination of conductivity plus the Peltier and Joule heating effects. The heat flux involved in the operation of the thermoelectric device consists of two parts: the conventional heat flux produced by the thermal gradient and controlled by the thermal conductivity of the thermoelectric material and the heat liberated by the electrical current in the device. The electrical current produces two heating effects, Peltier heating and Joule heating. The total heat flux is

$$q = \frac{k\Delta T}{\ell} + \alpha T_h I - \tfrac{1}{2} I^2 R \quad (1)$$

Under normal operating conditions, with the internal resistance of the device matched to the external load resistance for maximum power output:

$$I = V/2R \text{ and } V = \alpha\Delta T \quad (2)$$

so that

$$I = \frac{\alpha\Delta T}{2R}. \quad (3)$$

Equation 1 may be rewritten as

$$Q = qA = k_{te}\frac{A\Delta T}{\ell} + \frac{\alpha^2 T_H \Delta T}{2R} - \frac{\alpha^2}{4R}(\Delta T)^2 \quad (4)$$

or, since $R = \frac{\ell}{\sigma A}$,

$$Q = k_{te}\frac{A\Delta T}{\ell} + \left(\frac{\alpha^2 \sigma T_H}{2\ell}\right) A\Delta T - \frac{\alpha^2 \sigma A}{4\ell}(\Delta T)^2 \quad (5)$$

and

$$Q = \left[k_{te} + \left(\frac{\alpha^2\sigma}{2}\right) T_H - \left(\frac{\alpha^2\sigma}{2}\right)\frac{\Delta T}{2}\right]\frac{A\Delta T}{\ell} = k_{eff}\frac{A\Delta T}{\ell}. \quad (6)$$

Thus, the thermal processes in the thermoelectric device can be represented by the temperature-dependent effective thermal conductivity, $k_{eff}$.